



## **Digitalisation of condition monitoring data as input for fatigue evaluation of wheelsets**

Downloaded from: <https://research.chalmers.se>, 2024-03-13 10:30 UTC

Citation for the original published paper (version of record):

Maglio, M., Asplund, M., Nielsen, J. et al (2019). Digitalisation of condition monitoring data as input for fatigue evaluation of wheelsets. Proceedings of the XIX International Wheelset Congress

N.B. When citing this work, cite the original published paper.

# Digitalisation of condition monitoring data as input for fatigue evaluation of wheelsets

Michele MAGLIO<sup>1</sup>, Matthias ASPLUND<sup>2</sup>, Jens C O NIELSEN<sup>1</sup>,  
Tore VERNERSSON<sup>1</sup>, Elena KABO<sup>1</sup>, Anders EKBERG<sup>1</sup>

<sup>1</sup>CHARMEC, Chalmers University of Technology, Gothenburg, Sweden

<sup>2</sup>Trafikverket, Luleå, Sweden

michele.maglio@chalmers.se

matthias.asplund@trafikverket.se

jens.nielsen@chalmers.se

tore.vernerson@chalmers.se

elena.kabo@chalmers.se

anders.ekberg@chalmers.se

## Abstract:

A field test in which a train was run at different speeds over an impact load detector is described. One of the wheelsets in the train had severe wheel tread damage. The results are presented and the relation between the speed of the train and the magnitude of the impact loads registered for the two wheels is discussed. The defects on the wheel tread have been studied and scanned by means of 3D laser and their characteristics are described. An in-house software for the simulation of dynamic wheel–rail interaction has been improved by including the possibility to account for the cross-coupling of the two wheels within the same wheelset. The contact algorithm and a possible implementation of discrete defects in the in-house software are discussed. The in-house software gives, among other possible outputs, the maximum dynamic loads occurring at both wheels of the wheelset. To show an example of the utility of such information, fatigue analyses for the axle are performed for the different running conditions used during the field tests. The impact loads measured on the day of the tests are given as input to the fatigue analyses.

**Keywords:** wheel tread damage, impact loads, wheel–rail dynamics, rolling contact fatigue, wheel flats, RCF clusters

## 1. INTRODUCTION AND SCOPE

Wheel tread damage leading to unacceptably high vertical dynamic wheel–rail contact forces is a major cause of train delays in large parts of the Swedish railway network, in particular during the coldest months of the year [1]. According to regulations, vehicles generating contact forces exceeding the allowed wheel–rail impact load limit have to be taken out of service. This may cause major disruptions in the schedule of railway operations. Impact loads generated by wheel tread imperfections, such as wheel flats and rolling contact fatigue (RCF) clusters, result in high stresses in wheels, axles and bearings, thus increasing the risk of fatigue failures [2]. In addition, overloads due to such wheel tread defects may shorten the life of track components, such as rails and sleepers, resulting in higher costs for maintenance of infrastructure. Different forms of wheel out-of-roundness (OOR) can also cause increases in rolling noise, impact noise and ground-borne vibration [3].

A study aiming to specify temperature-dependent alarm limits based on simulations of dynamic vehicle–track interaction and rail crack propagation is performed in [4]. That study accounted for several operational parameters, such as thermal stresses and bending moments in the rails, which are in turn dependent on other factors such as train speed and axle distance, etc. The study only considered the maximum impact load and did not distinguish between wheels affected by RCF and wheels with wheel flats.

A significant difference exists in the way wheel flats and RCF clusters are developed. The first type of tread damage forms in a limited amount of time, usually due to locked brakes resulting in sliding between the wheel and the rail, while the latter is the result of a gradual process caused by frictional wheel–rail contact [5]. RCF usually initiates in a specific location of the tread. If a cluster of cracks is generated, it starts affecting larger parts of the wheel circumference. This may cause severe material fall-out from the wheel tread.

Within the frame of a project led by Trafikverket (the Swedish transport authority) and SJ (the Swedish national railway operator), the loads generated by a damaged wheel passing over an impact load detector at different speeds were measured with the aim of investigating the relation between the train speed and the load response [1]. More details about this field test are given in Section 2. The measured loads will be used to validate an in-house software for the simulation of dynamic vehicle–track interaction. This software is capable of computing the contact loads acting between the wheels and the rails for different types of wheel and rail surface damage [6]. The theory behind the software, its implementation and the developed capabilities will be briefly described in Section 3.

The calculated load spectra can be used to compute stresses generated in wheelsets subjected to wheel tread damage. Using these stresses to identify the resulting fatigue life of the wheelset axle is a powerful tool for the design and maintenance planning of wheelsets, see Section 4.

## 2. MEASUREMENT OF WHEEL–RAIL IMPACT LOADS

The field test introduced in Section 1 was performed in April 2018 at a site called Sunderbyn on the Iron Ore line in the northern part of Sweden, where one of the impact load detectors managed by the Swedish transport authority is located. At the time of the test, the detector consisted of eight instrumented sleepers, each of which was equipped with two load cells. The detector was calibrated in April 2017 [1]. The wheel profile, the rail profiles and the relative lateral and vertical displacements between wheel and rail were also measured at the detector.

### 2.1. Damage characterisation

The test featured a bidirectional train composed of three units: two locomotives (one for each traffic direction) and a passenger coach in the middle. One of the wheels of the passenger coach had generated loads that previously

exceeded the alarm limit at another detector [1]. This wheel was severely affected by wheel tread damage, see Figure 1. In particular, one of the two wheels was characterised by the presence of several RCF clusters on the wheel tread. The size, distribution and depth of these clusters were non-uniformly varying over the running surface. The opposite wheel on the axle was not showing such serious forms of damage. However, some minor wear was present as well as several rounded indentations which were expected to give only a minor influence on the measured load magnitudes [5].



Figure 1 – Left: Section of the tread surface of the less damaged wheel. Rounded indentations and some minor wear are visible. Right: Section of the tread surface of the damaged wheel where two of the main RCF clusters are located.

The OOR of the two wheels were measured manually and the tread profiles were measured both manually and by using a laser measuring device installed in the detector. No remarkable results were collected for the less damaged wheel, while the tread surface of the other wheel could be described by two damaged areas located on diametrically opposite sides. Each area was characterised by the presence of two major RCF clusters, whose depths reached values of up to 1.8 mm. In addition several minor defects existed. The same wheel was also characterised by an ovality of 0.2 mm [1].

In the manual measurement, the tread surfaces of both wheels in the damaged wheelset were scanned using a portable 3D optical laser scanner HandySCAN connected to the commercial software VXinspect [7]. This equipment has a maximum measurement accuracy of 0.03 mm, which allows for a very detailed characterisation of the RCF clusters. The scans could afterwards be post-processed in the software VXmodel and exported into a commercial CAD software. These detailed scans were performed with the aim of accurately modelling the geometry of each RCF defect in the simulation of dynamic vehicle-track interaction, see Section 3.

## 2.2. Field test results

On the day of the field test, the damaged wheelset was carrying an axle load of 14.4 tonnes, corresponding to a static load of 7.2 tonnes acting on each wheel [1]. The bidirectional train was run in both directions over the impact load detector without being turned around. In other words, the wheel affected by the RCF damage was always impacting on the same side of the detector (the side named “right” in the detector internal reference system). Seventeen

trials were performed, three at speed 10 km/h, seven at 55 km/h, six at 100 km/h and one at 140 km/h [1].

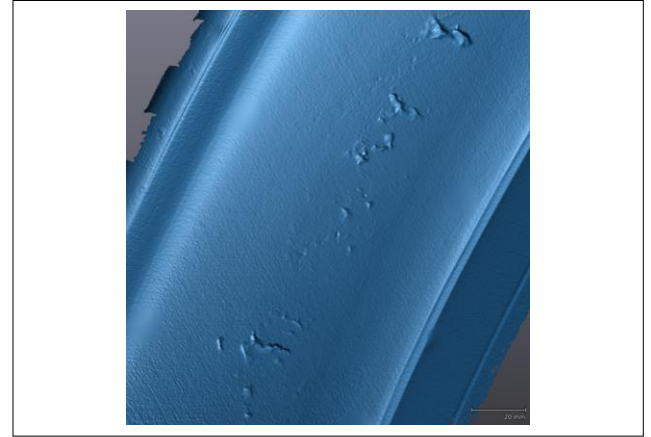


Figure 2: A detail of the post-processed geometry of the most damaged wheel. The RCF clusters visible in this figure are the same as those shown in the right picture of Figure 1.

For each trial, the speed of the train, the time of the day, the mean load magnitude and the peak impact load magnitude generated by the passage of the two wheels were recorded [1]. When analysing the detector data, the mean load corresponds to the static load acting on the wheel, whereas the peak load is the maximum registered vertical contact force. The dynamic load is given by the difference between the peak and the mean loads. The results from the experiments can be seen in Figure 3, where data related to each of the two wheels are connected by linear interpolation.

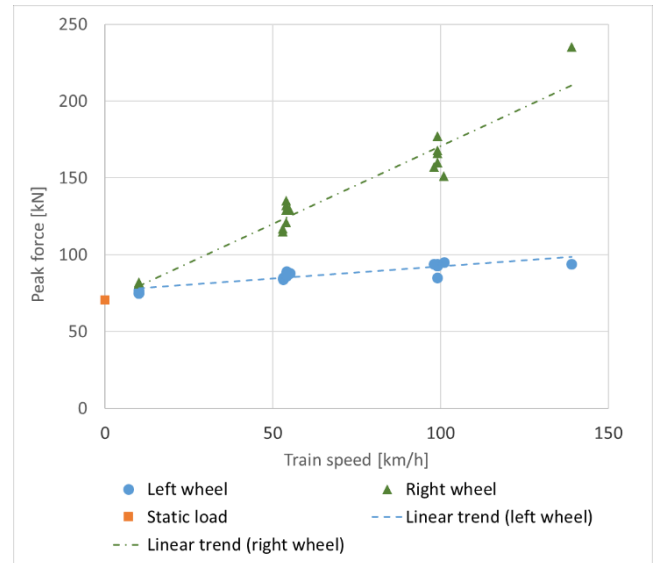


Figure 3: Peak loads measured during the field test in Sunderbyn in April 2018. The most damaged wheel is referred to as “right wheel”, whereas the other one is named “left wheel”

The peak loads registered for the most damaged wheel (“right wheel”) show a linear increase of about 0.95 kN per km/h increase in train speed. A much less pronounced linear growth in peak loads (0.20 kN/(km/h)) was recorded for the opposite wheel, (“left wheel”). The effect on the left wheel may either be due to the cross-coupling within the wheelset or to some minor form of damage (e.g. the observed small indentations). As for the mean loads, their values showed no dependency on speed, as expected. A single additional trial

was performed at 140 km/h. The results from this trial did not fully match the linear trend shown in Figure 3.

### 3. SIMULATION OF DYNAMIC VEHICLE-TRACK INTERACTION

The employed computer program is a software for simulation of dynamic vehicle–track interaction developed at Chalmers, see [6]. A large number of functions and capabilities have been implemented in the software throughout different research projects, e.g. [8] and [9]. The software was validated against another simulation model for dynamic vehicle–track interaction (DIFF) in [10]. DIFF in turn was validated against full scale test results [12].

#### 3.1. Convolution integral approach

The simulation of dynamic vehicle–track interaction is carried out in the time domain using a convolution integral approach. The influence of discrete wheel tread irregularities on the non-linear wheel–rail contact (including situations with loss of and recovered wheel–rail contact) is considered while keeping a low computational cost [11]. This approach has also been applied for the simulation of noise from tyre–road contact [13].

In the time domain, the dynamics of the wheel is represented by its Green’s function, which is the inverse Fourier transformation of the wheel receptance computed in the frequency domain. The track is modelled by means of moving Green’s functions, which describe the displacement response at a point of the rail that is moving away from the excitation point at the speed of the train. This means the motion of the contact point is taken into account. The track model consists of a pair of 60 kg/m rails resting on 70 sleepers with a spacing of 0.60 m.

The displacements of the wheel  $\xi_W$ , see Eq. (1), and of the rail  $\xi_R$ , Eq. 2, as a function of time are obtained by convoluting the respective Green’s functions  $G_W$  and  $G_R$  with the time-variant normal contact force  $F^N$ . Note that  $G_R$  in Eq. (2) is a moving Green’s function and is therefore dependent on the train speed  $v$ .

$$\xi_W(t) = \int_0^t F^N(\tau) G_W(t - \tau) d\tau \quad (1)$$

$$\xi_R(t) = \int_0^t F^N(\tau) G_R(v\tau, t - \tau) d\tau \quad (2)$$

#### 3.2. Contact formulation

The normal contact problem is solved by using the active set algorithm proposed by Kalker [14]. It is assumed that the wheel and rail can be approximated by two elastic half-spaces. At the interface between the two bodies, a potential contact area is defined. This area is discretised into a mesh of rectangular elements. The distance between the wheel and the rail is computed with respect to the centre of each element. If the distance is negative, indicating an overlap, the contact pressure is computed. The procedure of computing the distance and the contact pressure is repeated until all the elements in contact have zero displacement and a positive pressure value. If a negative displacement occurs for some elements (i.e. bodies are intersecting), the procedure is iterated again [11].

The tangential contact problem is based on Kalker’s transient rolling contact model [14]. The contact area is divided into a stick zone and a slip zone. The local tangential

displacements are calculated by summing the displacements from the previous time steps and the shift given by the effect of creepages [11].

Discrete irregularities, for example wheel flats [15] and rail squats [8], as well as other types of surface irregularities, such as rail corrugation, can be added to the contact formulation. In future work, the different geometrical characteristics of the defects could be parameterised to study the effect of different potential shapes of irregularities on the rolling contact behaviour.

#### 3.3. Wheelset model

In order to account for non-symmetric distributions of damage between the two wheels (as in the case of the field tests discussed in Section 2) and to allow for non-symmetric loading, as well as for developing and testing non-symmetric wheelset designs, the cross-coupling effect of the two wheels mounted on the same axle was implemented in the simulation model. This implies that the dynamic response of one wheel does not just depend on the contact force acting on that wheel, but also on the load occurring in the contact located on the opposite wheel of the wheelset. A similar problem where the cross-coupling effect was considered for two rails within a railway turnout has previously been dealt with, see [9].

The cross-coupling effect can be accounted for by extracting receptances at both nominal contact points of the wheelset in a Finite Element (FE) dynamic simulation. The frequency response function computed at one contact point when a unit load is applied in the same position is referred to as the direct receptance, whereas, for the same load case, the frequency response function computed at the contact point on the other wheel is referred to as the cross-receptance.

In this implementation, the displacement  $\xi_W^1$  of the contact point on wheel 1 is computed by solving two integrals. The first one convolutes the contact force  $F^1$  acting on the studied wheel and the Green’s function  $G_W^{1,1}$  computed from its direct receptance. The other integral convolutes the contact force  $F^2$  acting on the other wheel and the Green’s function  $G_W^{1,2}$  computed from the cross-receptance, see Eq. (3).

$$\begin{aligned} \xi_W^1(t) = & \int_0^t F^1(\tau) G_W^{1,1}(t - \tau) d\tau + \\ & + \int_0^t F^2(\tau) G_W^{1,2}(t - \tau) d\tau \end{aligned} \quad (3)$$

The receptances used in the current work have been computed using the commercial software Abaqus [16] from a 3D solid model of the symmetric wheelset used by Trafikverket in the field test. The FE model was meshed with 8232 hexahedral (C3D8R) and 840 triangular prism (C3D6) linear 3D stress elements with reduced integration (Figure 4). The primary vertical suspension was modelled by adding a spring with 10.5 kN/mm stiffness in parallel with a viscous damper having a damping coefficient of 50 kNs/m on a central node of both axle journals.

The receptance (vertical displacement per unit force as a function of frequency) plots for the two nominal contact points were extracted with a subspace steady-state dynamic analysis for the frequency interval 0–1000 Hz, see Fig. 5. The characteristic modes that were identified in Abaqus occurred within the frequency intervals predicted for non-

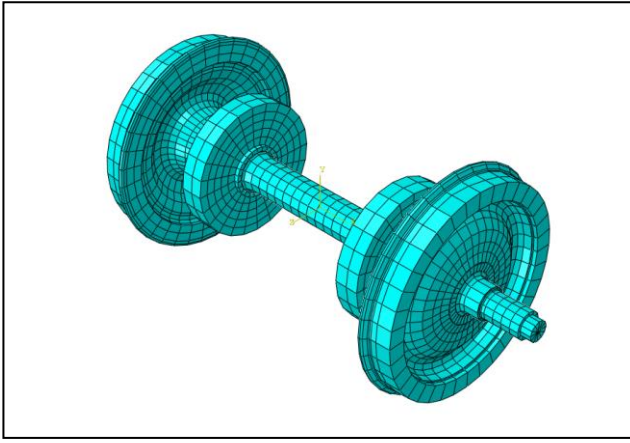


Figure 4: FE model of the wheelset used during the field test in Sunderbyn

powered wheelsets in [17]. A sensitivity analysis proved that including the dynamic behaviour of the wheelset at frequencies higher than 1000 Hz did not cause significant changes in the computed impact loads.

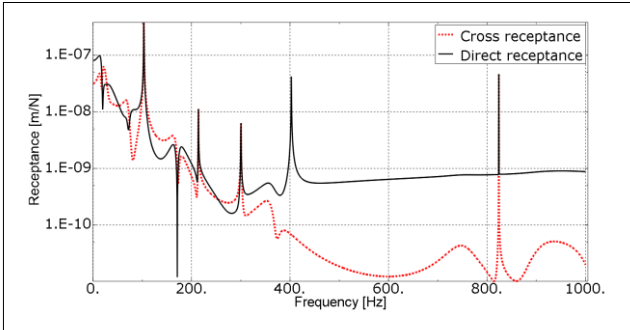


Figure 5: Direct and cross receptance magnitudes for the wheelset model shown in Fig. 4 computed using Abaqus.

#### 4. IMPACT LOAD ASSESSMENT AND FATIGUE ANALYSES

The irregular geometries of the observed wheel tread defects were approximated in order to fit regular shapes that could be described by analytical formulations. The geometric parameters of the main defects (i.e. depth, length, width, longitudinal position on the wheel tread and lateral position with respect to the rolling circle) were obtained from the captured 3D scans. The results of the simulations will be presented at the IWC2019 conference.

##### 4.1. Fatigue analysis procedure

The in-house dynamic vehicle–track interaction software can be used in the design phase of wheelset components when combined with a dynamic FE model. For example, the calculated impact loads can provide input in subsequent fatigue evaluations considering the dynamics of the wheelset to assess new axle designs or they can be employed to estimate optimal maintenance intervals for wheelsets affected by damaged wheels.

There is a broad variety of procedures and standards that can be followed to accomplish these aims. In the present work, the loads measured by the impact load detectors during the field test described in Section 2 have been used to study the fatigue resistance of some sections of the axle in the damaged wheelset. A simplified quasi-

static approach based on the European standard EN 13103:2009 [18], for design of non-powered axles, has been used to highlight the importance of the vertical loading. To this end, the load case of curved track (given in the EN standard) is complemented with a straight track load case and the stress results of these are combined with additional stresses introduced by the impact load. The dynamic loads (i.e. the difference between the maximum detected impact loads and the static load acting on the corresponding wheel) obtained during the field test at different speeds are summarised in Table 1. The carbody centre of gravity was assumed to have a height of 1000 mm with respect to the centre of the wheelset, and the axle load used during the field tests was employed. The effect of braking was neglected in the current study.

Table 1: Results from measurement of dynamic wheel–rail impact loads using the detector described in Section 2.

Train speed [km/h]	0	10	55	100	140
Dynamic load [kN]	0	11	55	95	165

The calculations were first performed for the cases of 1) a train in a curve and 2) a train on tangent track (not considering impact loads). The forces and moments are computed according to the standard. Starting from those values, the state of stress is computed for relevant sections of the axle and compared to the maximum stresses (100 MPa for seats on the axle and 166 MPa for the remaining axle body, assuming axle steel grade EA1N [18]).

In a second stage, the dynamic load magnitudes listed in Table 1 were added to the wheel–rail contact force acting on one wheel (thus ignoring that a dynamic factor is implemented in [18]). The increased magnitude of the contact load transmitted by the loaded wheel was compensated by reaction forces on the axle journals. In this way, the dynamic impact was simplified and treated as a quasi-static load case. However, in future work, dynamic finite element analyses will be performed and the effect of the extra loading, as well as of the detailed geometry of the axle, will be considered in order to extract more refined stress results.

##### 4.2. Fatigue analysis results

In the case of operations on a curved track and no extra dynamic loads coming from wheel tread damage, the stresses witnessed in the most critical sections are significantly below the maximum values given in [18], see Table 2. As the speed increases and additional dynamic loads are accounted for, the stresses increase for these critical sections. The numerical results show that fatigue may occur below the wheel seat at a train speed of 140 km/h. Such a prediction may however be conservative, since curving will lead to a lateral shift of the rolling circle. This means that the wheel–rail contact will be shifted away from areas with substantial tread damage and the dynamic loads on the wheelset will be lower.



Table 2: Results from the fatigue analyses for the most critical sections of the axle when the train is running on a curved track.

Section	Stress [MPa] witnessed at the given train speed [km/h]					Max stress [MPa]
	0	10	55	100	140	
Wheel seat	59.5	62.7	75.8	87.7	108.7	100
Fillet near brake disc	93.4	97.9	115.7	132.0	160.8	166

When considering running on a tangent track the fatigue stress results are given in Table 3. When not accounting for any extra dynamic loads, the most critical section is located at the fillet area near the brake disc. When speed increases, other sections suffer more the effects of the dynamic loads. At 100 km/h, the most critical sections are at the collar groove and at the wheel seat (since the latter has a lower fatigue limit due to the fretting contact with the wheel hub). However, according to the model described above, fatigue is not initiated when the damaged wheelset is running on tangent track, not even when the dynamic impact load registered at 140 km/h is used in the calculation (there is still a 10% margin for initiation of fatigue in the collar groove).

Table 3: Results from the fatigue analyses for the most critical sections of the axle when the train is running on a tangent track.

Axle section	Stress [MPa] witnessed at the given train speed [km/h]					Max stress [MPa]
	0	10	55	100	140	
Collar groove	45.8	52.7	80.3	105.5	149.5	166
Wheel seat	35.4	38.5	51.1	62.9	83.7	100
Fillet near brake disc	59.6	63.8	81.1	97.1	125.5	166

## 5. CONCLUSIONS

A new method for the simulation of dynamic interaction between a wheelset and a railway track has been described. The influence of discrete wheel tread defects on wheel–rail impact loads and resulting stresses in the wheelset can be studied. The flexible wheelset model used in the simulation is based on a detailed FE model accounting for the various wheelset components including brake discs and axle boxes. Results from simulations will be discussed at the IWC2019 conference. In this paper, a simplified fatigue calculation has been carried out based on the European standard and using measured impact loads as additional input.

## ACKNOWLEDGEMENTS

The current work is part of the activities within the Centre of Excellence CHARMEC (CHAlmers Railway MEchanics, [www.chalmers.se/charmec](http://www.chalmers.se/charmec)). Parts of the study have been funded within the European Union's Horizon 2020 research and innovation programme in the project In2Track2 under grant agreement No. 826255.

The efforts put by Trafikverket, SJ AB and in particular Pär Söderström in performing the field tests, as well as the support given by Dr Peter Torstensson with the coding activities in the in-house software are gratefully acknowledged.

## REFERENCES

- [1] Asplund M. Provkörning med hjulskada över hjulskadedetektor (in Swedish), Technical report, Trafikverket, Luleå, Sweden, 18 pp, 2018.
- [2] Andersson R. Squat defects and rolling contact fatigue clusters – Numerical investigation of rail and wheel deterioration mechanisms, PhD thesis, Chalmers University of Technology, Department of Industrial and Materials Science, 2018.
- [3] Nielsen J, Johansson A. Out-of-round railway wheels – a literature survey, Proceedings of the Institution of Mechanical Engineers, vol 214, pp 79-91, 2000.
- [4] Ekberg A, Kabo E & Nielsen J, Allowable wheel loads, crack sizes and inspection intervals to prevent rail breaks, Proceedings of the 11th International Heavy Haul Association Conference (IHHA 2015) Perth, Australia, pp 30–38, 2015.
- [5] Deuce R. Wheel tread damage – an elementary guide, Technical report 100115000, Bombardier Transportation GmbH, Germany, 38 pp, 2007.
- [6] Torstensson P, Squicciarini G, Krüger M, Nielsen J, Thompson D. Hybrid model for prediction of impact noise generated at railway crossings, Book section, Notes on Numerical Fluid Mechanics and Multidisciplinary Design, Springer-Verlag, pp 759-769, 2018.
- [7] VXiinspect and VXi model, Creaform, Canada <https://www.creaform3d.com/en>.
- [8] Andersson R, Torstensson P, Kabo E, Larsson F. The influence of rail surface irregularities on contact forces and local stresses, Vehicle System Dynamics, vol 53, pp 68-87, 2015.
- [9] Li X, Nielsen J, Torstensson P. Simulation of wheel–rail impact loads and measures to reduce differential track settlement in railway crossings, Chalmers University of Technology, Department of Mechanics and Maritime Sciences, submitted for publication, 2018.
- [10] Andersson R, Torstensson P, Kabo E, and Larsson F. An efficient approach to the analysis of rail surface irregularities accounting for dynamic train–track interaction and inelastic deformations. Vehicle System Dynamics, 53(11):1667–1685, 2015.
- [11] Pieringer A. Time-domain modelling of high-frequency wheel/rail interaction, PhD thesis, Chalmers University of Technology, Department of Civil and Environmental Engineering, 107 pp, 2011.
- [12] Nielsen J. High-frequency vertical wheel–rail contact forces— Validation of a prediction model by field testing. Wear, vol 265, pp 1465-1471, 2008.
- [13] Andersson P. Modelling interfacial details in tyre/road contact – Adhesion forces and non-linear contact stiffness, PhD thesis, Chalmers University of Technology, Department of Civil and Environmental Engineering, 107 pp, 2005.
- [14] Kalker J. Three-dimensional elastic bodies in rolling contact. Kluwer Academic Publishers, Dordrecht, Boston, London, 1990.
- [15] Pieringer A, Kropp W. A fast time-domain model for wheel/rail interaction demonstrated for the case of impact forces caused by wheel flats, Proceedings of Acoustics '08, Paris, France, 2008.
- [16] Simulia, Abaqus 6.14-2 User's guide.
- [17] Chaar N. Wheelset structural flexibility and track flexibility in vehicle-track dynamic interaction, PhD thesis, Royal Institute of Technology, Stockholm, 52 pp, 2007.
- [18] Svensk standard SS-EN 13103:2009+A1:2010 Railway applications – Wheelsets and bogies – Non-powered axles – Design method. SIS Swedish Standards Institute, 56 pp, 2010.

## Author information



First(Main) author: Michele M. Maglio  
 Title: PhD Student  
 Research Field: Railway Mechanics  
 Contact Address: [michele.maglio@chalmers.se](mailto:michele.maglio@chalmers.se)